

Design of Ceramics Heater for Stirling Engine

Teruyuki AKAZAWA*¹, Koichi HIRATA*², Takeshi HOSHINO*³, Hideki KITA*⁴
and Kazuhito FUJIWARA*⁵

- *1 The Japan Society for Design Engineering Member, estir Co., Ltd.
800 Tsutsui-cho, Yamato Koriyama City, Nara 639-1123, JAPAN
akazawa@estir.jp
- *2 Full member, National Maritime Research Institute
6-38-1, Shinkawa, Mitaka-shi, Tokyo 181-0004, JAPAN
khirata@nmri.go.jp
- *3 Non-member, Japan Aerospace Exploration Agency
7-44-1 Jindaiji Higashi-machi, Chofu-shi, Tokyo 182-8522, JAPAN
hoshino.takeshi@jaxa.jp
- *4 Non-member, Nagoya University Graduate School of Engineering
2266-98 Anagahora, Shimo-Shidami, Moriyama-ku, Nagoya, Aichi 463-8560, JAPAN
hkita@nuce.nagoya-u.ac.jp
- *5 Non-member, Kumamoto University Graduate School of Science and Technology
2-39-1 Kurokami, Kumamoto 860-8555, JAPAN
fujiwara@kumamoto-u.ac.jp

Abstract

Free piston Stirling engines with integrated linear alternators have the compact size and high conversion efficiency for the sake of the simplicity of mechanical movements. These engines have been developed with the conversion efficiency of 25%. The material property of ceramics heater is critical in order to achieve such high efficiency. In this paper, the successful design process of the ceramics heater is described. Temperature and stress of the ceramic heater have been calculated by the method of thermo-fluid dynamical analysis and the proper dimensions were decided. Several types of test products have also been designed and manufactured for the evaluation of actual efficiency. Heater efficiency of 63% was estimated from the analysis and the actual test data on free piston engine. It was concluded that the use of ceramics heater in Stirling engine is promising and the high performance of the engine can be realized.

Keywords: Stirling engine, free piston Stirling engine, ceramics heater, silicon carbide

1 Introduction

The Stirling engine was invented in 1816 by Robert Stirling, a clergyman from Scotland. This was the boom period for steam engine boilers, but these often exploded and there was demand for a safe engine. The Stirling engine is an external combustion engine operated by gas, such as air, helium or nitrogen. Several thousand were manufactured in the mid-19th century and used as a source of power for water pumps and machine tools. At that time, the thermal efficiency of these engines was low with an internal charge air pressure of around 1MPa and a heating temperature of around 500°C. By the end of the 19th century they almost disappeared due to the development of steam engines and the emergence of internal combustion engines.

In the 20th century, the Dutch company, Philips, turned their attentions to quiet external combustion engines and developed the compact, high-output and highly efficient Stirling engine by using various fuels and the working gases, helium and hydrogen. Many engines were developed from compact, single cylinder engines with an output of several kW and large 4 cylinder engines with an output of 265kW and were installed in portable generators that use various fuels as well as in automobiles and boats. However, in run tests conducted mainly in America in which engines were installed in vans, running fuel efficiency only improved to a level somewhere between a gasoline-powered vehicle and a diesel-powered vehicle. As a result, the commercialization of these engines for vans was shelved.

From 1980, these Stirling engines with high efficiency [1] as shown in **Figure 1**, were used as stationary engines in Japan and momentum increased to develop them as a solution for the problem of air pollution caused by exhaust gas from automotive engines. From 1982 to 1987, the “Research and Development into a General-purpose Stirling Engine” project was implemented by the then Ministry of International Trade and Industry as part of the Moonlight Project. This project was implemented by public research organizations led by the New Energy Development Organization (NEDO) and several private companies and concentrated on the development of a utilization system concerned with the practical development of engines with 3kW and 30kW outputs and of heat pumps.

In the aforementioned project development, many expensive heat-resistant metal pipes made from inconel and hastelloy were used in the heater section, which is exposed to high temperatures, in order to provide high thermal efficiency and the complex construction was

comprised of structures welded to the heater head section, etc. This caused issues from a cost perspective and commercialization proved difficult.

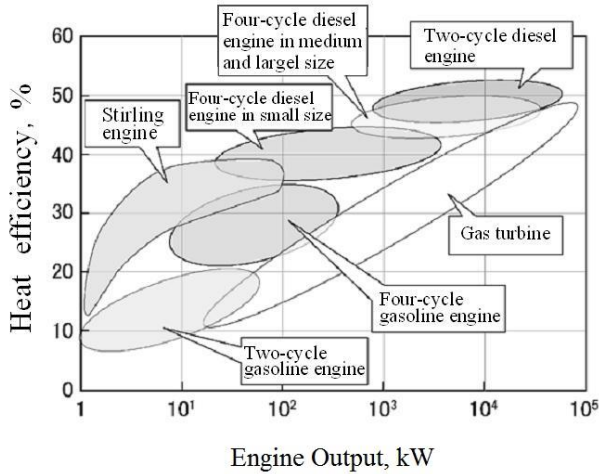


Fig.1 Heat efficiencies of typical engines [1]

In this paper, we describe how we use fine ceramics for the heater section of the engine, which is exposed to high temperatures, to design and develop a ceramic heater with a simple integrated structure that also maintains high thermal efficiency. Further, we provide an example of an actual free piston Stirling engine that uses this heater [2] to [3] and discuss the effectiveness.

2 Ceramic material suitable for heaters

2.1 Basic principles of a Stirling engine

Figure 2 shows a schematic of a beta form Stirling engine. A Stirling engine is an external combustion engine with superior characteristics, such as high thermal efficiency and the ability to use a variety of heat sources. From the perspective of achieving the ideal heat cycle including regeneration heat exchange, this thermal efficiency is consistent with the theoretical thermal efficiency of the Carnot cycle represented by low temperature heat sources and high temperature heat sources. However, because a Stirling engine is based on the principle that heat is transferred in an isothermal process, it has the qualities of a high efficiency engine at low output as shown in Figure 1. In order to utilize the characteristics of the Stirling engine high efficiency heat engine, it is beneficial to increase the temperature of high-temperature reservoir of the working gas.

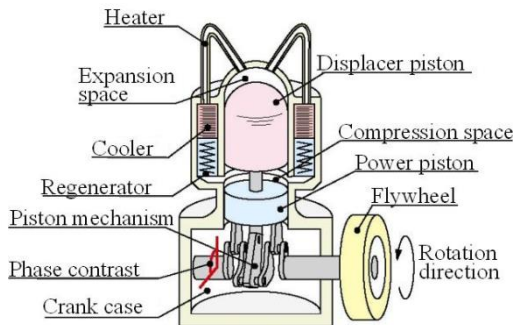


Fig.2 Schematic of Stirling engine

2.2 Selecting materials for the ceramic heater

Ceramic materials can be used under higher temperature conditions compared to general metal materials and therefore it is possible to increase the high temperature heat source by using ceramic materials for the heater material. In so doing, it is possible to increase the thermal ratio of the high temperature heat source relative to the low temperature heat source and increase the thermal efficiency. However, in order that they can be used as heater materials, ceramic materials need to meet the requirements of a high-temperature and high-pressure vessel that is resistant to high pressure and impact at high temperatures and selecting and configuring the shape of the materials is difficult and thus far has not been achieved. Further, because helium gas is used as a working gas for increasing efficiency in the case of Stirling engines, it is also a requirement to select materials that can withstand internal pressure in compact substances and low-strain materials as regards thermal stress. Candidate materials include silicon carbide, silicon nitride, zirconia and alumina, but silicon carbide, which has high thermal conductivity, is the strongest candidate from the perspective of heater heat transfer performance and silicon nitride is the strongest candidate in terms of strength and workability. Because the manufacturing method of both materials is different, two types of material are produced; reaction-sintered body and normally-sintered body. When choosing a material from these candidates, we referred to the paper by Itano *et al.* [4] Other manufacturing methods exist, namely hot press sintering and hot isostatic pressing (HIP), but these were not included as candidates here because of the low degree of freedom in the shape and the high cost. First, we prioritized increasing thermal efficiency and selected silicon carbide as the first candidate material and with the strength and reliability required for future mass production in mind, we chose silicon nitride as the second candidate material. We conducted a basic heating strength test. We discussed our final material selection based on these test results. We decided to use silicon carbide because we found that it exhibited thermal conductivity three times greater than that of silicon nitride, because it can be manufactured using normal sintering at a low cost, and because it meets the required design strength. Hereafter, we describe the performance of a normally sintered silicon carbide product.

2.3 Silicon carbide oxidation evaluation test

A heater is affected by oxidation during use and therefore it is necessary to consider the effect that oxidation has on material strength at the design stage. We conducted an accelerated oxidation test by setting the heater wall temperature higher than the envisaged usage temperature of 800°C. Material strength is evaluated using the bending strength after the oxidation test, but in order to consider the conditions on the surface and inside the heater separately, we cut out and used 4 mm wide, 3 mm thick and 30 mm long test pieces from both the sintered surface and the inside of the material. We conducted oxidation processing for both the ceramic test piece taken from the surface (represents the surface of the heater) and the machined

test piece taken from the inside (represents the inside of the heater) and heated the ceramic test piece at 1200°C for 2 hours using a gas burner so that the oxidation effect was clearly apparent, and heated the machined test piece in an electric furnace for 2 hours at 1200°C and 1400°C. The gas burner provides a strong oxidative effect because the flame contains water vapor.

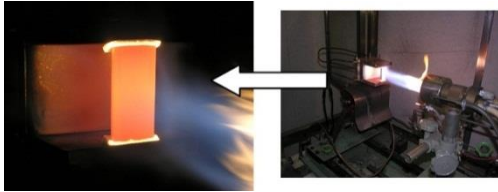


Fig.3 SiC test piece in burner oxidation

Table 1 The effect of burning on the fracture stress of as-sintered test pieces

Burning temperature: 1200°C
Test method : Four-point bending test

Conditions	Before burning	After burning
Average fracture stress (MPa)	472±80	546±45
Weibull modulus, m	5.9	13.1
Fracture stress at 0.1% failure probability (MPa)	156	335

Table 2 Fracture stress of as-machined test pieces at high temperature

Test method : Four-point bending test

Temperature	RT	1200°C	1400°C
Average fracture stress (MPa)	343±67	386±56	394±31
Weibull modulus, m	5.6	6.6	14.3
Fracture stress at 0.1% failure probability	108	144	251

Figure 3 shows oxidation processing using a gas burner. A reduction in the depth of evenness on the surface of the samples was apparent for both the sample heated by the gas burner and the sample heated in the electric furnace and it was ascertained that oxidation was in process. After oxidation processing, we allowed the samples to cool at room temperature and then evaluated the deterioration using a 4-point bending test with an upper span of 30 mm and a lower span of 10 mm. **Tables 1** and **2** show the test results expressed as a Weibull plot using the median rank method. If we compare the strength of the ceramic test piece and machined test piece before oxidation, the average strength (maximum principal stress: 472MPa) and the Weibull modulus that represents the strength reliability (m:5.9) of the ceramic test piece are both higher than the same characteristics of the machined test piece (343MPa, m:5.6). It is clear that both the average strength and the Weibull modulus of the ceramic test piece were improved as a result of oxidation processing using a gas burner. Even contrast, even though both the average strength and Weibull modulus of the machined test piece improved as the processing temperature

increased to 1200°C and 1400°C, the increase was small when compared to the ceramic test piece after oxidation processing. If we consider these results, we can conclude that the strength of the machined test piece is inferior to that of the ceramic test piece because of the fine cracks left by machining and the effect of this is particularly significant on silicon carbide, which has low fracture toughness. Therefore, particular care should be taken when machining sintered product in the secondary process. Further, the reason why the strength of both sintered pieces increased after oxidation processing is assumed to be because the shape and size of surface defects are changed by oxidation. It is thought that this change in surface property is dependent on temperature.

We ascertained from the above results that the strength of silicon carbide does not deteriorate due to oxidation, but actually increases. We will advance current ceramic heater design using the data obtained for the material properties.

3 Preliminary study of ceramic heaters

3.1 Ceramic heater design conditions

Using simulation [5], the combustion gas temperature is converted from a combustion temperature of 2000°C to a high temperature housing temperature (helium gas temperature) of an estimated 600°C via the heater and the average gas pressure is estimated at 2.5MPa. It is possible to create a thermal design for the target generating output from these research findings and estimated values of efficiency for each section. The pressure resistance design pressure on the ceramic heater was set to 5MPa with a safety factor of 2. When designing the strength of the heater, it is necessary to estimate the design strength of silicon carbide. Taking into consideration the safety factor including impact load, we set the design strength to the fracture stress at 0.1% failure probability value of 108MPa shown in **Table 2**. We set the heater unit target performance to 70% using the efficiency of converting the combustion gas from the inlet temperature of 2000°C to the high temperature housing temperature of 600°C.

3.2 Heating test using a heater unit for evaluation

We conducted a heating test using an engine for evaluation as a test of proof stress against the thermal stress from the heater unit. **Figure 4** shows the structure of ceramics heater for test. Many conventional metal heaters are comprised of dozens of heat transfer tubes, but this heater is comprised of a combustion gas heat transfer part that receives heat from the combustion gas passing through the fan, a flat plate that manages pressure resistance strength and a working gas transfer part that provides heat to the working gas through a number of small holes. Each part is machined to a complex shape. We checked for defects caused by the thermal stress generated when heat was applied.

Figure 5 shows the external appearance of the silicon carbide heater after heating for 100 hours at 950°C. We were able to verify that no cracks or fractures had been generated and that the heat had not caused any particular problems as regards the machined shape. [6]

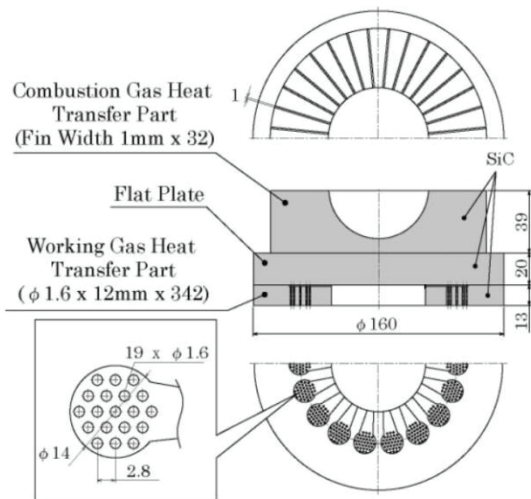


Fig. 4 Structure of ceramics heater for test



Fig. 5 Ceramics heater

3.3 Effect of fastening parts to the periphery of the heater

The heating test in the previous section produced favorable results, but because the heater initially designed and trialed had three component parts fastened to the periphery, when gas pressure was applied to the inside of the Stirling engine, large bending stress was generated particularly when the thickness of the central part of the heater was thin. Therefore, we used a convex-shaped structure in which the thickness was greater in the central vicinity. Figure 6 shows the analysis results of ceramics heater.

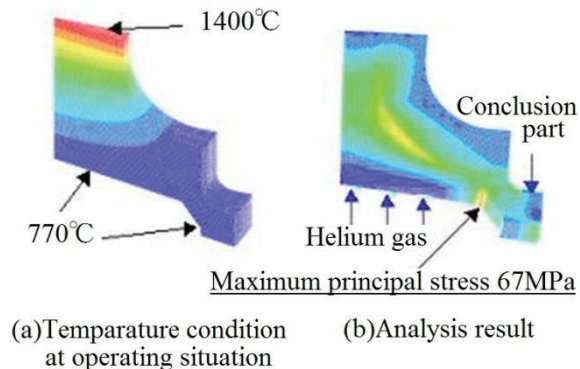


Fig. 6 Analysis results of ceramics heater

If the internal pressure of the helium gas is estimated at 5MPa and the combustion gas inlet temperature at 2000°C for the simulation, the temperature of the upper

surface wall of the heater becomes 1400°C and the temperature of the side walls 770°C. The maximum principal stress is 67MPa. There should be no issues because this value is below the design strength of 108MPa, but in the pressure test the heater fractured at an internal pressure of 3.5MPa. When parts are fastened to the periphery of the heater, the heat is prevented from transferring by the fastening members and therefore several ring-shaped heat insulating members and metal members are attached to the periphery. It was established that, as a result, a non-uniform part occurs in the arced insulating member and a fracture starting point is easily generated. Consequently, we changed the fastening method to form a surface supported by a central integrated columnar heat insulating member ensuring that it is difficult for non-uniformity to occur.

4 Analysis of thermal fluid around the heater

Figure 7 shows the configuration of two typical types of heater and the heater specifications are shown in Table 3. Further, the configuration when the heater is mounted on the engine is shown in Figure 8. In type (A) part of the expansion chamber is built into the inside of the silicon carbide heater. In contrast to (A), in type (B), the expansion chamber and ceramic heater are completely separate structures. In this case, it is possible to separate the combustion gas and helium gas (He) and reduce the heater thickness to the working limit.

Table 3 Main heater dimensions

Dimension / Shape	Internal Pipe			External Fin			Material
	Bore (mm)	Length (mm)	Number	Width × Height	Length (mm)	Number	
A	2	25	120	1 × 13	50	60	SiC
B	2	65	32	1 × 44	50	32	SiC

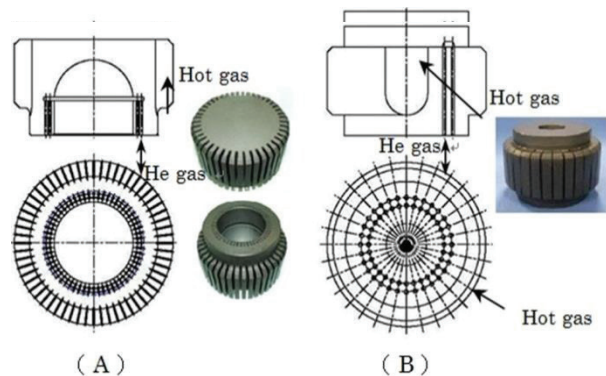


Fig. 7 Main heater configurations

According to the results of the thermal fluid analysis for the heater unit, the maximum principal stress for heater type (A) is 98MPa and for heater type (B) is 65MPa. The maximum principal stress for heater type (B) is 34% less because the main structure is separate from the expansion chamber. The unit efficiency of the heater compared to the target efficiency of 70% is 61.2% for heater type (A) and 63.4% for heater type (B) and the effect of the small partition wall thickness (approximately 1 mm) of type (B) is apparent. We

decided to use heater type (B) based on strength and efficiency. [7] **Figure 8** shows the upper engine configuration of (B) type.

Once we had decided on the heater structure, we conducted thermal fluid analysis for the heater including the working gas. We used the ratio of the working gas thermal dose to the amount of heat entering the heater from the high temperature heat source (combustion gas) as a measure of the heater's unit efficiency and evaluated the heater performance using this as an indicator.

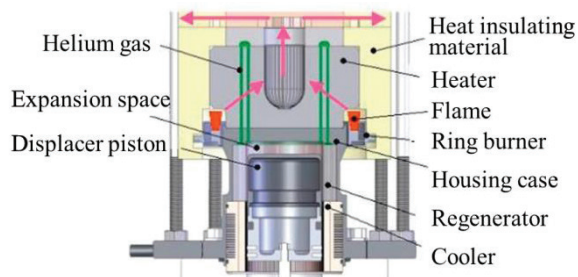


Fig.8 Upper engine configuration –(B) type

We included the heat exchange connected to the heater, the heat insulating material installed to the top of the heater and the holding parts in the simulation model. The analysis results are shown in **Figure 9**.

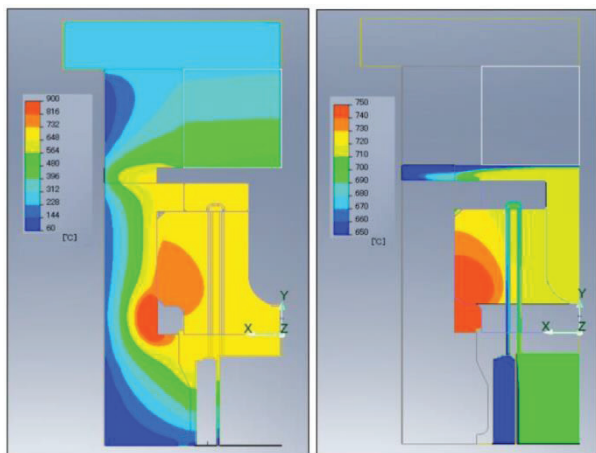


Fig. 9 Analysis result–(B) type

The temperature distribution for the solid parts, including engine peripheral parts, and the gas parts are shown separately. According to these results, the heater unit efficiency is 61.3%. This is significantly lower than the efficiency of a heat exchanger used in boilers, etc. but if the temperature of the expansion space is kept below the high-temperature condition of 600°C, this is generally an appropriate value for achieving target performance.

5 Validating the effectiveness using an actual engine

Lastly, we installed a ceramic heater into an actual free piston type Stirling engine to verify the

effectiveness of the heater. **Figure 10** shows the prototype of free piston Stirling Engine with SiC heater. A conventional kinematic type Stirling engine needs to be connected to a rotating generator that converts reciprocal motion into rotational motion using mechanisms, such as cranks and cams, which means that the whole machine increases in size and issues such as the generation of mechanical loss in the transfer mechanism arise. In contrast, the free piston type Stirling engine does not need cranks, etc. and therefore the engine generator as a whole can be kept compact and also increased efficiency can be expected because of the reduction in mechanical loss [8]. This can be achieved by attaching a direct-drive linear generator [9] to [10] to the piston. However, there is a chance that efficiency will deteriorate because the phase difference between the displacer and piston cannot be set accurately.

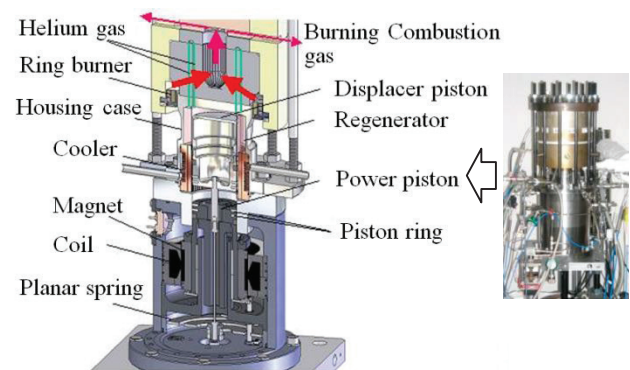
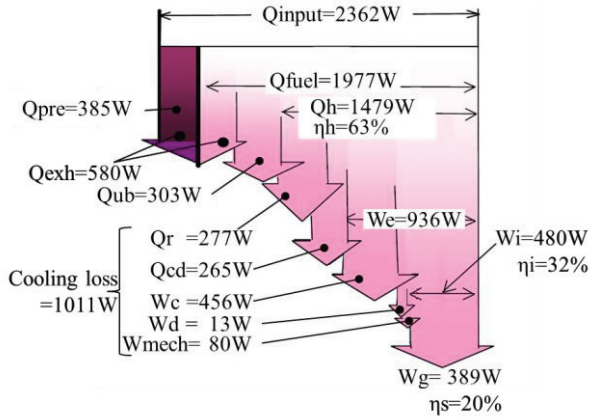


Fig. 10 Prototype of free piston Stirling engine with SiC heater

Figure 11 shows the energy balance of this engine. Q_{fuel} represents the fuel heat input expended by the town gas under the burner and Q_{pre} represents the quantity of preheated air taken in from the exhaust gas and preheated for combustion. Q_{input} is the total energy heat input and is the sum of Q_{fuel} and Q_{pre} . The quantity of heat supplied to the high-temperature reservoir via the heater is expressed as the quantity of effective heat input, Q_h , and the ratio with total heat input Q_{input} is the heater efficiency η_h . As predicted in the thermal fluid analysis, the maximum temperature difference at the heater wall surface is less than 50°C and the effect of using silicon carbide material, which has good thermal conductivity, is clear. Further, the heater efficiency η_h is 63%, which is by and large the same as the simulation results.

In terms of performance indicators for the Stirling engine, we evaluated the total quantity of exhaust gas heat Q_{exh} , the quantity of burner heat loss Q_{ub} as well as the cooler cooling loss, the reheat loss within the heat exchanger Q_r , and the heat conduction loss Q_{cd} . Of these, the cooler cooling loss calculated from the temperature difference at the inlet and outlet for the water cooled by the cooler and the flow amount is approximately 1kW, which is not an insignificant value. However, the indicated heat cycle efficiency η_i solved from the effective heat input Q_h and the indicated horsepower W_i is shown as 32%, which means that high efficiency for a free piston type engine was achieved.

The power output, W_g , does not account for mechanical loss W_{mech} or generator loss and is measured using a wattmeter. A power output W_g of 389W is obtained with this engine (a gross thermal efficiency η_s of 20%) and is of a sufficient level for practical use from a performance perspective.



Q_{input}	Total energy heat input	W_e	Expansion space input
Q_{fuel}	Fuel heat input	W_c	Compression space loss
Q_{pre}	Preheated air input	W_i	Indicated horsepower
Q_h	Heat input	W_d	Windy loss
Q_{exh}	Exhaust gas heat loss	W_{mech}	Mechanical loss
Q_{ub}	Burner heat loss	W_g	Power output
Q_r	Heat exchanger loss	η_h	Heater efficiency.
Q_{cd}	Heat conduction loss.	η_i	Heat cycle efficiency
η_s	Gross thermal efficiency		

Fig. 11 Energy balance of engine

5 Conclusion

In this study we designed a ceramic heater suitable for a Stirling engine and obtained the following findings.

- 1) By using silicon carbide material as the material for a Stirling engine heater we realized a heat converter capable of withstanding high-temperature combustion temperature conditions that cause difficulties for metal heaters.
- 2) We set the design stress as the principal stress at 0.1% failure probability, 108MPa, which we obtained from the basic test results on silicon carbide strength.
- 3) For this test we conducted a heating test on a heater for evaluation and verified that there were no issues, such as cracks or fractures, under heating high-temperature conditions of 950°C.
- 4) We found that, unlike with metal heaters, particular care is required as regards fastening methods when using ceramic heaters.
- 5) We were able to produce a detailed design, which included the heater shape, using thermal fluid analysis of the heater and peripheral components.
- 6) In trials on an actual machine using a ceramic heater we obtained favorable results; a heater efficiency of 63%, an indicated efficiency of 32% and a power output of 389W, which highlighted the commercial viability.

Acknowledgements

We would like to add that part of this study was

conducted by way of a study commissioned by the New Energy and Industrial Technology Development Organization, "Developing a Next Generation Engine using a Ceramic Heat Converter and a New Type Linear Generator," and we would like to express our deepest gratitude to those concerned and to collaborators in this research.

References

- [1] Keiji Murao, Teruyuki Akazawa, Koichi Hirata, Takeshi Hoshino: "Development of a High-efficiency Stirling Engine", Collected papers from the 9th Japan Society of Mechanical Engineers Stirling Cycle Symposium, (2005), pp. 105-106.
- [2] Teruyuki Akazawa, Keiji Murao, Koichi Hirata, Takeshi Hoshino, Hideki Kita: "Development of a Cogeneration Stirling Engine for Household Use", Collected papers from the 10th Japan Society of Mechanical Engineers Stirling Cycle Symposium, (2006), pp. 103-104.
- [3] Takeshi Hoshino, Shoichi Yoshihara, Teruyuki Akazawa, Keiji Murao: "Prototype of Free Piston Stirling Converter for Household Use", Proceedings of Journal of Power and Energy Systems, Vol. 2, No. 5, (2008), pp. 1232-1235.
- [4] Hisao Itano, Yukiyasu Asano: "The Automotive engineering Series: Ceramics for Automotive Use", Sankaido Publishing, (1987), pp. 105-108.
- [5] Iwao Yamashita, Kazuhiro Hamaguchi, Noboru Kagawa, Koichi Hirata, Yutaka Momose: "Stirling Engine Theory and Design." Sankaido Publishing, (1999), pp. 34-37.
- [6] Koichi Hirata, Yoshiyuki Imai, Eiko Ishimura, Masakuni Kawada, Teruyuki Akazawa, Keiji Murao: "Development of a Stirling Engine for Evaluation of a Ceramic Heat Exchanger." Collected papers from the 10th Japan Society of Mechanical Engineers Stirling Cycle Symposium, (2006), pp. 105-108.
- [7] Teruyuki Akazawa, Koichi Hirata, Yasuyuki Imai, Eiko Ishimura, Masakuni Kawada: "Development of a Stirling Engine for Evaluation of a Ceramic Heat Exchanger." Japan Society of Mechanical Engineers National Convention summary papers, Japan Society of Mechanical Engineers, (2006), pp. 136-137.
- [8] Teruyuki Akazawa, Keiji Murao, Yukihiro Okada: "Development of a Linear generator for a Free Piston Stirling Engine", Collected papers from the 9th Japan Society of Mechanical Engineers Stirling Cycle Symposium, (2005), pp. 33-34.
- [9] Takeshi Hoshino, Shoichi Yoshihara, Teruyuki Akazawa, Keiji Murao: "Performance Testing the New Type Linear Generator", Collected papers from the 10th Japan Society of Mechanical Engineers Stirling Cycle Symposium, (2006), pp. 109-112.
- [10] Takeshi Hoshino, Shoichi Yoshikara, Teruyuki Akazawa, Keiji Murao: "400W Free Piston Stirling Generator", Collected papers from the 11th Japan Society of Mechanical Engineers Stirling Cycle Symposium, (2007), pp. 21-24.

Received on November 26, 2013

Accepted on January 28, 2014